AB

IPNO-DRE 98-15

Evidence for narrow dibaryons at 2050, 2122 and 2150 MeV observed in inelastic pp scattering

B.Tatischeff[1],J.Yonnet[1],M.Boivin[2],M.P.Comets[1], P.Courtat[1],R.Gacougnolle[1],Y.Le Bornec[1], E.Loireleux[1],F.Reide[1] and N.Willis[1]

[1] *Institut de Physique Nucleaire Orsay* sw9907
F-91406 Orsay Cedex,France

[2] *Laboratoire National Saturne CEA-DSM CNRS-IN2P3*
F-91191 Gif-sur-Yvette Cedex,France

Submitted to Physical Review C

Evidence for narrow dibaryons at 2050, 2122 and 2150 MeV observed in inelastic pp scattering

B. Tatischeff[1], J. Yonnet[1], M. Boivin[2], M. P. Comets[1], P. Courtat[1],
R. Gacougnolle[1], Y. Le Bornec[1], E. Loireleux[1], F. Reide[1],
and N. Willis[1],

[1] *Institut de Physique Nucléaire, CNRS/IN2P3, F-91406 Orsay Cedex, France*

[2] *Laboratoire National Saturne, CNRS/IN2P3, F-91191 Gif-sur-Yvette Cedex, France*

The reaction p p $\Rightarrow$ p $\pi^+ X$ was studied in order to look for dibaryons at invariant masses M_{pX}. The experiment was performed at three different energies (T_p=1520, 1805 and 2100 MeV) and at several different angles from 0° up to 17° (lab.). Narrow dibaryons were observed in invariant mass spectra at 2050, 2122 and 2150 MeV. The corresponding numbers of standard deviations vary between 3.2 and 13.1. The mass of these narrow dibaryons agree with systematic studies of dibaryonic masses experimentally observed through many experiments performed by various collaborations. Such a systematic study allows us to define the mean dibaryonic mass spectrum which is in agreement with the spectrum calculated within a simple phenomenological mass formula based on color magnetic interactions between two colored quark clusters.

PACS numbers: 14.20.Pt, 13.75.-n, 12.40.Yx

I. INTRODUCTION

The experimental search for narrow dibaryons is an essential task for several reasons. Such dibaryons, if their existence is confirmed, is a crucial argument to decide whether or not physics at a few GeV can be entirely explained by baryonic and mesonic degrees of freedom, or if additional assumptions such as quark degrees of freedom, must also be considered. Over the last 20 years, many results have been obtained from experiments (not always carried out with the highest precision) that have led some authors to conclude, that they have observed such structures - whereas others reach the contrary conclusion. It is therefore highly desirable to reach a conclusion concerning the existence of these narrow dibaryons, regardless of their origin.

The main reason for the unceasing debates related to the existence of narrow dibaryons is the smallness of their signatures compared to the superimposed physical background of baryons and mesons in

interaction for masses larger than the pion production threshold mass (2014 MeV). For these studies, the useful experiments needed to be as precise as possible.

Such a precise experiment was performed using a proton beam. The reaction p p $\Rightarrow$ p $\pi^+ X$ was studied in order to look for the dibaryonic M_{pX} invariant mass simultaneously with the study of missing mass M_X whose results were presented elsewhere [1] [2]. Here the missing mass can be either one neutron (exclusive measurement), or N π . The experiment will be described in the next paragraph. The results will then be presented and discussed. A review of the results from several experiments studied previously will be presented. Finally an attempt to interprete these results will be presented, followed by a discussion describing other possible interpretations.

II. EXPERIMENT

The experiment was performed at the Saturne synchrotron using the Spes3 facility. The beam energies were 1520, 1805 and 2100 MeV. The beam flux varied between 10^8/burst and $5 * 10^8$/burst, depending on the spectrometer angle (and incident energy), in order to keep the acquisition dead time to less than 10%. The liquid H_2 target of 393 mg/cm^2 was held in a container with Ti windows having a thickness of 130 μm . External heat shields comprised of Al 24 μm thick were placed in the beam-line on either side of the target. The effect of these windows was checked by regular empty target measurements. The corresponding countings were small, typically $< 5\%$. We therefore deduced that the target windows were not a source of noticeable contamination. We also deduced that although our measurements were performed at small angles, the data was not contaminated by any hot areas of incident beam which could have been scattered by some mechanical piece at the entrance of the spectrometer. The Spes3 spectrometer properties were described elsewhere [3]. To summarize its main properties, that it is a mean value solid angle spectrometer ($\pm$ 50 mrd in both the horizontal and vertical planes), and secondly that it is a large momentum range spectrometer ($600 < pc < 1400$ MeV). Both particles were detected in the same set-up consisting of several drift chambers. The information from these detectors was used to reconstruct the trajectories. The first chamber was localized on the focal plane of the spectrometer and was followed by several chambers that were lying orthogonal to the particle trajectories. The trigger consisted of four planes of plastic scintillator hodoscopes. The time of flight baseline from the first to the last scintillator was 3 m. The dimensions of each plastic detector were 12*40 cm^2 for the first plane, and 18*80 cm^2 for the last plane. Each of these two planes consisted of 20 scintillators. Since mean-timers and constant fraction discriminators were used, the time resolution for each scintillator was typically $\sigma = 180$ ps. An energy loss measurement was taken from the first plane of scintillators, and was mainly used to discriminate between one and two charged particles. The large horizontal angular magnification

of the spectrometer produced a large horizontal angular opening (up to 30^0) of the trajectories at the output of the spectrometer. It resulted in a large number of possible combinations (132), between the first and last scintillation counter planes, requiring the same number of coincidences. Careful calibrations and efficiency measurements were performed between all 132 channels.

Since both particles, p and π^+ were analyzed by the same detector elements, events were lost when both their trajectories intersected on each plane of the detection system (drift chamber or trigger hodoscope). A simulation code was written in order to correct such lost events. For M_{pX} invariant masses ($M_X > M_n$) the correction function was a smooth function varying between 1.1 and 1.3. For $M_X = M_n$, the correction function was also smooth except in a narrow range of invariant masses, when both trajectories intersected on the focal plane. The data for these last invariant masses was removed in order to avoid introducing a spurious oscillation due to this correction. The normalizations of the number of events, were performed using two telescopes in view of the target, and an ionisation chamber located in front of the beam catcher. The information of these detectors were normalized by ^{12}C activation measurements.

A second time of flight between both particles was used in order to eliminate the random coincidences and possible wrong identifications coming from real pp $\rightarrow$ ppX events. A correction was made to take into account the differences in trajectory lengths, and then a common window of $\pm$ 2 ns was used for all these times of flight channels. When the data reduction code associated a wrong assignment of the trigger and chamber information (0.6% of events), the corresponding information was removed.

Special care was taken to ensure that no bias could be produced by particles originating from scattering on mechanical pieces at the entrance of the spectrometer. A detailed discussion of this part of the analysis was presented in reference [1]. A simulation code was written in order to study the consequences of particles scattered by the target in the vertical plane at angles $50 \leq |\phi| \leq 80$ mrd. No narrow structure appeared in M_{pX} invariant masses which could have been attributed to such bias.

The beam polarizations were .78, .74 and .70 for the three increasing energies. The polarities were reversed after each spill in order to avoid any bias due to slow polarization drift.

III. RESULTS

A. General presentation

The raw data obtained at T_p=1805 MeV, $\theta = 0.75^0$ (lab.) before any correction or normalization, is shown in Fig.1. This figure represents the scatter plot of the missing mass, M_X, versus the invariant mass, M_{pX}. In the figure, software cuts were applied to M_X. In order to suppress a very intense line corresponding to p $\pi^+ n$ reaction, we selected events for $M_X > 960$ MeV. The blank line corresponds

to the area where the p and π^+ momenta are the same, as mentioned previously. The external cuts are due to p and π^+ momenta limits at 600 and 1400 MeV/c respectively. The three intense regions correspond to :

- $M_X \approx$ 960-1000 MeV and $M_{pX} \approx$ 2150 MeV. This is a remaining tail from the pp $\rightarrow \Delta^{++}$ n reaction which is insufficiently cut in this figure and will be dicussed later.
- $M_X \approx$ 1200 MeV (Δ mass) and $M_{pX} \approx$ 2270 MeV. These events correspond to two delta productions : Δ^{++} and Δ^0. They are not genuine broad resonances in the dibaryonic system.
- The increase in intensity along the upper limit of the scatter plot is due to the non-linear transformation between the proton momenta and the missing masses.

Different corrections and normalizations were applied, with a corresponding increase of the errors depending on the precision of the following factors :

- detection cell efficiencies,
- dead time losses,
- normalization of the number of events by the incident proton flux,
- lost events due to trajectories that intersect in one of the planes of the detection system,
- normalization of the cross-sections to constant momenta acceptances : Δp_p and $\Delta p_{\pi+}$.

A major part of these corrections was quantitatively determined using a simulation code written for this purpose. Careful attention was paid to experimental biases which could have been produced by some discontinuity in the correction functions (last two corrections). Software cuts were introduced on M_X at a value large enough in order to avoid introducing a bias due to the n missing mass tail. The effect of such cuts can be anticipated from Fig.1 and is illustrated in Fig.2. The upper part shows the horizontal projection of Fig.1, with an important tail from residual Δ^{++} n reactions. There is a remaining peak which will be reduced after normalization to constant momenta, but a discontinuity will remain. This peak in dibaryonic M_{pX} masses disappears totally when a software threshold of 1050 MeV is applied to the missing mass spectra.

Our experimental cuts ($600 \leq p \leq 1400$ MeV/c) remain constant, but the behaviour of the range of the studied events in the M_X=f (M_{pX}) scatter plot, changes with incident energy. The tail of the neutron missing mass decreases with increasing energy. The intense pp $\rightarrow \Delta^{++}\ \Delta^0$ spot moves inside the range and is located totally inside our range at T_p =1805 MeV. Finally the empty line from $p_p = p_{\pi+}$ momenta is less inconvenient at higher energy, since it is located in a less central position in the M_X=f (M_{pX}) scatter plot.

B. Results at T_p=1520 MeV

In Fig.3, we see the M_{pX} dibaryonic spectra obtained at T_p=1520 MeV for neutron missing mass $930 \leq M_X \leq 960$ MeV and at all forward angles where the data was achieved with a good resolution and large statistics. At all angles, a narrow structure appears around 2050 MeV, straight lines are drawn at this value. Fig.4 shows the corresponding angular distribution extracted by using polynomials for the background and a gaussian peak for the structure. The numbers of standard deviations (S.D.) vary from 12.6 at 0° up to 4.9 at 9°. The mean value of the width is $\sigma \approx 12.6$ MeV. The dashed curve is only here to guide the eye.

For missing masses larger than the neutron mass ($M_X \geq$960 MeV), other checks were performed to make sure that the corrections applied could not be a source of false structures. They are illustrated in Fig.5 for T_p=1520 MeV at 2^0 :

- the correction for lost events were made for elementary surfaces in the scatter plot M_X=f(M_{pX}), as opposed to mean corrections which were made on the single variable M_{pX},

- a limited smooth area was arbitrarily selected, in order to avoid all eventual structured cuts. Such area is shown in part (a) of Fig.5 between both circle arcs.

The corresponding consequence on M_{pX} distribution is shown in part (b) of Fig.5. We see a structure around 2122 MeV (↓). Then the same analysis was performed, without selection of the range between both circle arcs. The resulting M_{pX} distribution is shown in part (c), which in turn shows again the same structure.

We conclude that the structure around M_{pX}=2120 MeV and $\theta = 2^0$ is a genuine dibaryon and not an experimental artifact. On the other hand, the broad peak observed around 2160 MeV is a part of the $\Delta - \Delta$ final state.

The cross sections for M_{pX} dibaryonic invariant masses, are shown in Fig.6. The data was regrouped in order to reduce the statistical errors. The limits on M_X were adjusted in order to cut all regions having experimentally "intense" or "weak" counting areas in the M_X=f(M_{pX}) scatter plot. Therefore all regions of non smooth corrections were eliminated. The range in M_{pX} dibaryonic mass is higher than previously discussed and does not explore the region below 2050 MeV. Also the statistics is smaller. At all forward angles, there is a structure at a mean mass value of 2122 MeV. Straight lines are drawn for this M_{pX} mass. Although these structures are seen at all four forward angles, they are not well defined and therefore no extraction of cross section was performed. There are also indications of structures at 2066 MeV (2^0), 2183 MeV (2^0) and 2170 MeV (9^0).

Since the experiment was performed using polarized proton beams, the analyzing powers were also measured. Fig. 7 shows the analyzing powers for the two missing mass data, for 1520 MeV incident

protons at 5 and 9 degrees, since there is no polarization for forward angles, and since the resolution and the counting rate spoil for larger angles.

Although the error bars are smaller for neutron missing mass data than for X=Nπ missing mass data, there is no indication, in the analyzing power results, of any structure at the masses where they appear in the cross sections. In the case of larger missing masses $M_X > M_n$, structures can be seen (with a not very large confidence level).

C. Results at T_p=1805 MeV

Similar checks as those described for T_p=1520 MeV data, were performed for 1805 MeV data. Inside the scatter plot M_X=f(M_{pX}) several selections were carried out with continuous and smooth corrections. None of them allowed us to extract a narrow and small dibaryonic structure. This is illustrated in Fig.8 where we see two large and broad peaks at masses close to Δ n and Δ Δ dominate the cross section. (Their masses are slightly lower than the nominal values, since there are cuts in the experimental range). We see that the Δ n tail remains in spite of the cuts introduced in order to eliminate it. Similar results were obtained at all angles between 0.75^0 and 13^0, with the distinctive result that the ratio of Δ n over background, decreases with increasing angle. We conclude therefore that the T_p=1805 MeV energy was not suited for the observation of narrow dibaryon structures in our experimental conditions.

D. Results at T_p=2100 MeV

At this energy, no measurement was performed at angles larger than 9° lab. The consequence of the large number of two deltas production events observed in missing mass M_X and invariant mass $M_{p\pi+}$ was that in M_{pX} dibaryonic mass a large maximum occured around 2300 MeV (not shown)

By using appropriate cuts defining smooth boundaries in the M_X=f (M_{pX}) scatter plot, it was possible to extract the cross sections, presented in Fig.9. A dibaryon at M_{pX}=2150 MeV (σ=11 MeV) was clearly extracted from polynomial background at forward angles 0.7^0 and 3^0, with respectively 8.1 and 5.5 numbers of standard deviations.

An extension of the cross sections at three angles between 2170 and 2270 MeV is shown in Fig.10. A smaller structure is present at all angles around 2230 MeV. Since the corresponding S.D. are $\leq$ 2.6, its existence is possible but not firm.

IV. REVIEW AND DISCUSSION ON PREVIOUS RESULTS

A large number of experiments were performed in order to search for narrow dibaryons. Some of the authors have not observed them, and therefore have concluded on their non existence. We will focus on the results where narrow dibaryonic structures have been observed and therefore advocated. Several results were obtained from bubble-chamber slides studies. They are of course low statistic experiments. Since they were reported in different occasions [4] [5], they will not be mentionned here. Our discussion therefore does not presume to be exhaustive. Some other precise experiments which will be recalled in the next paragraphs, were already mentionned previously with more details.

The aim of the following discussion is to recall several results, preferably the most recent ones.

A. Precise previous results in N-N elastic channel

1. pp elastic differential cross-sections.

Cross sections for pp elastic scattering were measured at COSY [6] in the range $2112 < \sqrt{s} < 2866$ MeV with bins which are equal to $\delta\sqrt{s} \sim 9.5$ MeV around $M_{pp} = 2122$ MeV. No structure was observed. The range of that study is marginal as compared to the range studied in our experiment.

2. $\vec{p}p$ elastic scattering analyzing powers.

Narrow structures were observed at KEK [7] [8] in the analyzing powers at the following invariant masses : 2160 MeV ($\Gamma_{1/2}$=14 MeV) and 2192 MeV ($\Gamma_{1/2}$=13 MeV). However very precise measurements were performed later at Saturne [9] using the Spes3 beam line and an energy degrader with variable thicknesses (rotating wheel). The large overlap between the results obtained from the Saturne experiment, for different extracted proton energies, allowed very precise relative adjustments. Such precaution is important since the $\gamma G = 3$ depolarization resonance occurs in this energy range. No structure was observed in the data of this Saturne experiment.

B. Precise previous results in inelastic channels.

1. Recall of some previous precise results concerning the dibaryon at 2122 MeV

A dibaryon was already observed at 2122 MeV from electronic and bubble chamber slide experiments. The $^3He(p,d)X$ reaction was studied at Saturne Spes1 beam line, some years ago, using electronics,

therefore with good statistical precision [11] [12]. The missing mass M_X had the following quantum numbers : T_X=1 and B_X=2. The experiment was performed at three energies : 750, 925 and 1200 MeV and several angles. Fig.11 shows some of these results with a number of standard deviations (S.D.) varying from 3.0 up to 6.9. The presentation of the results at T_p =750 MeV, θ=40^0 was changed since the first presentation [11], see [5].

The same reaction was studied at Los Alamos with polarized protons (T_p=800 MeV) [13]. The analyzing power data showed structures for several M_X close to our dibaryonic masses [11] [12].

The same situation occured for a dibaryon around 2190 MeV. It was observed with a good statistical precision using the $^3He(p,d)X$ reaction at Saturne and Los Alamos (same references).

2. The d' resonance.

A narrow dibaryon at 2060 MeV, has been advocated for several years. It was deduced [14] from pionic double charge exchange (DCX) reactions on several nuclei from ^{14}C to ^{48}Ca. This narrow dibaryon was supported by a recent result of DCX reaction study on ^4He performed at TRIUMF using the CHAOS spectrometer [15]. The existence of the d' resonance was confirmed in a two pions production reaction, namely the p p $\Rightarrow$ p p π^- π^+ reaction performed at ITEP [16] and at CELSIUS using a 750 MeV proton beam [17]. The experiment is similar to the one presented here, except that at Celsius, the energy was lower, the invariant $M_{pp\pi^-}$ mass was reconstructed, and a relatively narrow range of $M_{pp\pi^-}$ mass (2055 $\pm$25 MeV) was studied. A narrow peak at 2063 MeV (with a statistical significance of four sigmas), was found. This might be the same as the one which appears in our data at 2050 Mev (see Fig.3). A Status-Report concerning the d' searches in DCX and pp collisions was recently published [18]. Inside this paper, a table shows a list of various experiments with data analysis in progress. An enhancement at 2060 MeV (with a statistical significance of two sigmas), was observed in the $^4He(\pi^+,\pi^-pp)$ invariant mass search [19], studied at TRIUMF with 115 MeV π^+ beam.

Several theoretical calculations were performed in connection with this result [20] [21] [22] [23]. The d' isospin was anticipated as being even, and $J^P = 0^-$ since a very small width ($\Gamma_{\pi NN} \approx 0.5MeV$) was observed. This leads to the conclusion that the d' cannot decay into two nucleons. The two possibilities of isospin : 0 and 2, were investigated and discussed within the constituent quark model calculation (six quark system) [24] for a possible $J^P = 0^-$ dibaryon at 2065 MeV.

The first assignement of isospin 0, was supported by a QCD string model and three-body calculations and by non relativistic Fadeev equations with local potentials [25] (see several references inside). Using the resonating group model, the mass and wave function of a six-quark system of the d' ($J^P = 0^-$, T=0) was recently calculated [26]. Meanwhile isospin 2 was proposed [27], supported by the small experimental

width according to relativistic calculations and isobar model with first-order perturbation theory. The same isospin was proposed [28] using a nucleon-Δ interaction based on quark cluster model.

Of course, isospin 0 - which is presently preferred to isospin 2 [15] - is not excluded by our reaction. However our observed width for the dibaryon at 2050 MeV ($\sigma \approx 12.6$ MeV) is larger than the reported width of the d' ($\Gamma_{\pi NN} \approx 0.5$ MeV). Our experimental resolution (σ) for M_{pX} or M_{pn}, is estimated as being equal to 3.1 MeV at 0^0, and increases with increasing angle. Unless our structure observed at 2050 MeV in M_{pn} invariant mass corresponds to another dibaryon than the d', then the conclusion on the values of spin and isospin for this d' ($J^P = 0^-$, T=0), supported by the assumption of non coupling with the two nucleon channel, must be re-examined.

3. $pd \rightarrow \pi^- ppp$ experiment.

The invariant $M_{pp\pi^-}$ mass was studied using a 3300 MeV/c deuteron beam [29]. Two narrow enhancements were observed after quasi-free processes suppression at masses : 2199 $\pm$ 7 and 2258 $\pm$ 2 MeV. The first one compared favorably with the mass depicted on Fig.12 at 2191 MeV. An analysis based on impulse approximation reproduced correctly the shape of the distributions below the narrow peaks.

4. pd→pnp experiment.

The M_{np} invariant mass spectra from the pd→pnp reaction at 1000 MeV was studied [30]. Narrow dibaryons were extracted in the direct channel at 1950, 2020 and 2120 MeV. The two last masses fit precisely previous assignements (see Fig.12). The first mass has no counterpart on the same figure, although it is fair to admit that the experimental situation in this mass range is not clear.

5. $pn \rightarrow \pi^- pp$ reaction .

The invariant mass of two protons was studied using the pn→ π^-pp reaction [31] at ITEP (1980 MeV/c) protons. No narrow dibaryon was observed in this experiment, in the mass region $1890 < M_{pp} < 2170$ MeV.

6. $\pi^+ d \rightarrow pp$ reaction .

A precise $\pi^+ d \rightarrow$ pp experiment was performed to study an eventual structure in the energy dependence of this reaction [32]. Small steps in pion energy were used from 18 to 44 MeV, which corresponds to

$2032 < \sqrt{s} < 2056$ MeV. This is a very small energy range for dibaryon search (see Fig.12). Only one level is predicted inside that range, and it is located on the upper side at 2052 MeV. No structure was observed in that experiment.

7. $pp \rightarrow \gamma\gamma pp$ experiment.

The theory of this reaction was considered [33] [34], since it offers the advantage of allowing the study of narrow dibaryons with masses below the pion emission threshold (2014 MeV) where the probability of parasitic reactions is reduced. This two photons process is of course experimentally difficult due to the low counting rate. A narrow peak at 1923.5 ± 4.5 MeV with a statistical significance of 8σ was observed [35]. This value is close to 1916 MeV, which is a mass already reported in Fig.12. However the same reaction was recently studied at CELSIUS [36]. Narrow dibaryons were looked for in the mass range 1900 up to 1960 MeV. The authors concluded that their data presented no indication of a state in the 1917-1923 MeV range. However if several states actually do exist, separated by a few tens of MeV, the superposition of the corresponding peaks and their mirror peaks, could produce a flat distribution compatible with the results they show in Fig.3 implying a cross section lower than 50 nb.

8. $pp \rightarrow pn\pi^+$ experiment.

A precise kinematically complete pp→ $pn\pi^+$ experiment was performed near threshold [37]. The M_{pn} invariant mass varies between threshold (1878 MeV) and 1891 MeV for the largest incident energy. The aim of that experiment was not the study of dibaryons, and it is clear that such a small range is not suitable for such a study.

9. $\pi^- d \rightarrow \gamma X$ (X=$\pi^0 nn$, $\pi^- pn$) experiment.

It was performed at TRIUMF [38]. Pions at rest were stopped in D_2 in order to produce (π^- d) atoms. A transition from these atoms to neutral π^0nn or π^-pn could give a peak in the case of a sufficiently narrow dibaryon. However no peak was observed in the expected range of 10 to 20 MeV for γ ray, that is ± 5 MeV on both sides of 2002 MeV where a possible candidate was previously indicated from the $d(\pi^\mp, \pi^\pm)X$ experiment.

10. $\vec{p}p \rightarrow \pi^- X$ experiment.

It was performed at Saturne, Spes3 beam line at three energies : 1450, 2100 and 2700 MeV, in order to search for isospin T=2 dibaryons in the missing mass data [39]. One structure only at 2164 MeV was extracted ($\Gamma_{1/2}$ =15 MeV, S.D.=2.6). Since this mass is close to the M_Δ + M_N mass, it is difficult to eliminate a threshold effect. This mass value is the same as the mass of the structure observed in our experiment at T_p=1805 MeV.

C. Total and differential cross-sections and asymmetries for $\vec{p}$ p $\Rightarrow$ ppπ^0 reaction.

Although no enhancement was observed in these observables measured at Saturne [10], a simultaneous analysis of this data and of the results obtained previously from the np $\Rightarrow$ NN$\pi^\pm$ reaction, lead the authors to conclude that a strong possibility exists for a significant contribution of $^1D_2$ partial-wave in the isoscalar channel near $\sqrt{s}$=2129 MeV. This energy is the same as our peak mass of 2122 MeV, within the energy resolution of the pion production experiments . Our $\vec{p}$ p $\rightarrow$ p π^+X reaction allows isospin 0 and 1 (even 2). The same dibaryonic mass was observed previously in the $^3He(p,d)X$ reaction (already mentionned in 4B1) in an isovector channel. The fact that the same dibaryonic mass was observed in isospin channels 0 and 1, can be related to isospin degeneracy, predicted by some models which will be discussed later .

V. ATTEMPT TO DEFINE AN EXPERIMENTAL SET OF NARROW DIBARYONS.

Many experiments observed narrow structures in dibaryonic masses and concluded on their genuine existence. However only some amongst all these results had a statistical precision which allowed them to be conclusive. A part of those precise results was recalled in previous paragraphs. As was already noticed, the smallness of the signatures and their superposition above a large physical background, makes this work difficult. Therefore we compared all of the results in order to try to increase the confidence we could have on their genuine existence.

In an attempt to define which dibaryonic masses were observed with a reasonable confidence level, we have plotted on Fig.12 the masses of the narrow structures (vertical axis) reported by the authors whose references are displayed on the horizontal axis. Here the experiments performed with electronics are noted with squares and those from bubble chambers are noted with triangles. Full signs correspond to data with S.D.> 3.07 (confidence level > 99%), and empty signs for data with S.D.< 3.07. In some cases, the S.D. were not quoted by the authors but estimated from the published data. The observed

masses are not spread but concentrated around some values. These values are listed on the vertical scale and are called "experimental masses". The double line corresponds to ± 3 MeV, which can be considered as being an approximate precision for experiments performed with electronics.

VI. ATTEMPT FOR AN INTERPRETATION

More general than the study of dibaryons, the stability of exotic bound states of negative pions and neutrons was investigated [53]. Different theoretical papers deal with narrow dibaryons, either their existence, or their decay modes or the consequence of their hypothetical existence on some other observables. One consequence is the possibility of a Bose condensate of dibaryons occuring in nuclear matter [54]. Some works were performed within the Chiral Soliton Model [55]. The consequences of dibaryons on nuclear matter properties, or on the structure of neutron stars [56] [57] were considered. The inelastic production cross-section of d* (isoscalar $J^{\pi}=3^{+}$ didelta dibaryon) was calculated [58] and found to be in the μb/sr range, although it was not observed [59] in a d d $\rightarrow$ d X experiment. It's decay width into two nucleons was found to be in MeV's. It is not the aim of the present work to recall the various theoretical works which were devoted to dibaryon studies.

A. The phenomenological mass formula

Here we will present a very simple phenomenological relation, which nonetheless allows us to predict the observed "experimental masses" with a surprising accuracy.

The mass formula for two clusters of quarks at the end of a stretched bag was derived some years ago in terms of color magnetic interactions [60] :

$$M = M_0 + M_1[i_1(i_1+1) + i_2(i_2+1) + (1/3)s_1(s_1+1) + (1/3)s_2(s_2+1)]\,, \qquad (1)$$

where M_0 and M_1 are parameters deduced from mesonic and baryonic mass spectra and $i_1(i_2)$, $s_1(s_2)$ are isospin and spin of the first and second quark cluster respectively. We make the assumption that the clusters are $q^2 - q^4$. The spin and isospin values for a diquark (q^2) cluster are 0 or 1 and for a 4 quarks cluster (q^4) they are 0,1 or 2. We consider the two parameters M_0 and M_1 as being free and therefore we will also consider the formula as a phenomenological one. We first assume that the deuteron mass is obtained when $i_1 = i_2 = 0$, $s_1 = 0$ and $s_2 = 1$ [61], therefore giving the deuteron quantum numbers S=1, I=0. In this case $M_d = M_0 + (2/3)\ M_1$. We choose $M_0 = 1841$ MeV and $M_1 = 52.5$ MeV, in order to get the deuteron mass and the best agreement for the other masses. These parameters are about 12% lower than the corresponding values reported in [60]. The ratios between our values and those of

[60] are respectively 0.86 for M_0 and 0.89 for M_1. Couples of i_1 and i_2 allowing total isospins 0, 1 or 2, have to be considered if $M_X > M_n$ (otherwise total isospin=0 or 1). However if we restrict ourselves to dibaryonic masses below 2200 MeV, the calculated masses for isospin 2 do not introduce new levels, and the calculated masses for isospin 0 introduce only one additionnal level at 1911 MeV. Such results illustrate the strong degeneracy of the formula. The calculated mass spectra is shown in Fig.13. All the "experimental levels" are reproduced except for that at 1916 and 1902 MeV. From 2000 MeV to 2200 MeV the agreement with "experimental masses" is very good, with deviations $\leq$1 MeV. A similar good agreement between calculated masses using the same mass formula and recently observed narrow baryons was reached [1].

Angular distributions are needed to allow experimental spin determinations, for further comparison with the predictions (given in Fig.13), but the statistical precision has been too low up until now, to allow such studies.

B. The diquark cluster model.

A diquark cluster model for any multiquark system $q^k\bar{q}^h$ was developed by Konno et al. [62]. Amongst their different assumptions, let us recall the following : " Two quarks are strongly bound when they are in the same diquark cluster, if they are both in the $1s_{1/2}$ shell ". The non-strange dibaryon q^6 consists simply of three such diquarks, where all quarks are u or d. This model predicts the coexistence of broad and narrow resonances. It is a semi-phenomenological model since there are eight parameters determined using baryon masses and πd phase-shifts [62]. An agreement was found with broad dibaryon mass spectrum [63].

There were also other calculations based on the diquark model [64] and on the symmetry properties. This theory was applied mainly to exotic mesons or H dibaryon and not to non strange low mass dibaryons.

C. Are narrow dibaryons a consequence of narrow baryons recently observed ?

Narrow baryons were recently observed at low masses between neutron mass and Δ^0 mass, namely at 1004, 1044 and 1094 MeV [1]. Within the assumption that the narrow dibaryon masses are produced by all combinations of two baryonic masses (using the nucleon mass and the masses of the narrow baryons), we get a level sequence shown in the right part of Fig.14. The comparison with experimental dibaryons shows an agreement for several masses. Moreover the level density found is not very different from the experimental one.

VII. CONCLUSION

The pp $\rightarrow$ p π^+ X (X=n or N π) reaction was studied at the following three energies : 1520, 1805 and 2100 MeV and at several angles from 0 to 17^0 lab. In the invariant M_{pX} masses, several narrow dibaryons were observed at 2050, 2122 and 2150 MeV. These masses were compared to experimentally observed narrow dibaryons in previous experiments and were also compared to some phenomenological mass formulas. The agreement is good with narrow dibaryon masses observed in previous experiments.

The agreement with the phenomenological mass formula is noteworthy. When narrow **baryonic** masses are used to reconstruct the **dibaryonic** masses, the agreement is fairly good. The importance of such agreement lies in the simplicity of these approaches.

These results were also compared with the diquark model. We have found that the theoretical outline here is not as convincing with the observations as it was in the case of baryons.

During the data analysis a strongly excited broad structure was observed at 2300 MeV for 2100 MeV protons (not shown in the figures) and at 2270 MeV for 1805 MeV protons. These broad structures were associated with $\Delta^{++}\Delta^0$ dynamic resonant states and not with genuine dibaryons. Another broad structure was observed at 2170 MeV, and was associated with the Δ^{++} n dynamic resonant state.

At this time when the true existence of these narrow structures is becoming more and more confirmed, in spite of experimental difficulties due to the smallness of the signals, two questions arise :
- which conditions provoke the excitation of a specific dibaryonic mass in comparison with other dibaryonic masses in experiments where the range studied allows the observation of several dibaryons,
- what is the common origin of narrow **baryons** and narrow **dibaryons** observed nowadays. Some ideas were proposed. They have to be confirmed and a complete explanation has still to be done. All results concerning narrow dibaryons will be very useful for the study of color confinement at large distances.

ACKNOWLEDGMENTS

We wish to thank Dr. M. McCormick and Natalie Lutz for help in writing the English version of our paper.

---

[1] B.Tatischeff, J. Yonnet, N. Willis, M. Boivin, M. P. Comets, P. Courtat, R. Gacougnolle, Y. Le Bornec, E. Loireleux, and F. Reide, Phys. ReV. Lett. **79**, 601 (1997).

[2] J.Yonnet, B. Tatischeff, N. Willis, M. Boivin, M. P. Comets, P. Courtat, R. Gacougnolle, Y. Le Bornec, E. Loireleux, and F. Reide, Nucl. Phys. **A637**, 63 (1998).

[3] M. P. Comets, M. Boivin, Y. Le Bornec, E. Loireleux, B. Tatischeff, and N. Willis, IPN, Orsay Report No. IPNO DRE 88-41 (unpublished).

[4] B. Tatischeff, in *Proceedings of the XIIth Inter. Sem. on High Energy Physics Problems, Dubna, 1994.*

[5] B. Tatischeff, M. P. Comets, Y. Le Bornec and N. Willis in *Proc.Xth Int. Sem. on High Energy Phys. Problems, Dubna 1990,p. 177,World Scientific*, edited by A. M. Baldin, V. V. Burov and L. P. Kaptari.

[6] D. Albers *et al.*, Phys. ReV. Letters **78**, 1652 (1997).

[7] H. Shimizu *et al.*, Phys. ReV. **C 42**, R483 (1990).

[8] Y. Kobayashi *et al.*, Nucl. Phys. **A569**, 791 (1994).

[9] R. Beurtey *et al.*, Phys. Lett. **B293**, 27 (1992).

[10] G. Rappenecker *et al.*, Nucl. Phys. **A590**, 763 (1995).

[11] B. Tatischeff *et al.*, Phys.ReV. **C 36**, 1995 (1987).

[12] B. Tatischeff *et al.*, Europhysics Letters **4**, 671 (1987); Z. Physics **A 328**, 147 (1987).

[13] L. Santi *et al.*, Phys. ReV. **C 38**, 2466 (1988).

[14] R. Bilger, H. A. Clement, and M. G. Schepkin, Phys. ReV. Lett. **71**, 42 (1993); R. Bilger, H. A. Clement, and M. G. Schepkin, Phys. ReV. Lett. **72**, 2972 (1994); K. Föhl *et al.* Phys. ReV. Lett. **79**, 3849 (1997).

[15] J. Gräter *et al.*, Phys. Lett. **B420**, 37 (1998).

[16] L. S. Vorob'ev *et al.*, JETP Letters **59**, 77 (1994).

[17] W. Brodowski *et al.*, Z. Phys. **A355**, 5 (1996).

[18] R. Bilger, Nucl. Phys. **A629**, 141c (1998).

[19] R. Meier *et al.*, in *Proceedings of the 14th Inter. Conf. on Particles and Nuclei* (World Scientific, 1997) p. 368.

[20] A. Bobyk, A. Faessler and A. Kaminski, J. Phys. G : Nucl. Part. Phys. **23**, 375 (1997).

[21] R. Bilger, H. Clement, Th. Czarnecki, K. Fohl, B. Martemyanov, M. Schepkin, L. Vorobyev, and G. J. Wagner, Nucl. Phys. **A596**, 586 (1996).

[22] H. Garcilazo, J. Phys. G : Nucl. Part. Phys. **23**, 1101 (1997).

[23] K. Itonaga, A. J. Buchmann, G. Wagner, and A. Faessler, Nucl. Phys. **A609**, 422 (1996).

[24] G. Wagner, L. Ya. Glozman, A. J. Buchmann, and A. Faessler Nucl. Phys. **A594**, 263 (1995).

[25] H. Garcilazo, Phys. ReV. **C 56**, 1751 (1997).

[26] A. J. Buchmann, G. Wagner and A. Faessler, Phys. ReV. **C 57**, 3340 (1998).

[27] H. Garcilazo and L. Mathelitsch, Phys. ReV. Lett. **72**, 2971 (1994).

[28] E. Moro, A. Valcarce, H. Garcilazo, and F. Fernández, Phys. ReV. **C 54**, 2085 (1996); A. Valcarce, H. Garcilazo, and F. Fernández, Phys. ReV. **C 52**, 539 (1995).

[29] A. Deloff and T. Siemiarczuk, Z. Phys. **A 353**, 121 (1995).

[30] A. Deloff and T. Siemiarczuk, Nucl. Phys. **A555**, 659 (1993).

[31] B. M. Abramov *et al.*, Z. Phys. **C 69**, 409 (1996).

[32] E. A. Pasyuk *et al.*, Phys. ReV. **C 55**, 1026 (1997).

[33] S. B. Gerasimov, S. N. Ershov, and A. S. Khrykin, Phys. of Atom. Nuclei **58**, 844 (1995).

[34] V. L. Lyuboshitz and M. I. Podgoretsky, Phys. of Atom. Nuclei **59**, 262 (1996).

[35] V. M. Abazov *et al.*, JINR preprint E1-96-104.

[36] H. Calén *et al.*, Phys. Lett. **B427**, 248 (1998).

[37] J. G .Hardie *et al.*, Phys. ReV. **C 56**, 20 (1997).

[38] S. Stanislaus, D. S. Armstrong, D. F. Measday, P. Weber, and M. Harston, Phys. Lett. **B219**, 237 (1989).

[39] N. Willis *et al.*, Phys. Lett. **B229**, 33 (1989); M. P. Combes-Comets *et al.*, Phys. ReV. **C 43**, 973 (1991).

[40] B. Tatischeff *et al.*, Phys. Rev. **C 45**, 2005 (1992).

[41] O. B. Abdinov, A. A. Baireamov, Yu. A. Boudagov, Yu. Ph. Lomakin, A. A. Mailov, V. B. Fliagin, and Yu. N. Khargeev, JINR preprint P1-88-102, in Russian.

[42] N. Angelov *et al.*, JINR preprint P1-88-905; S. A. Azimov, K. G. Gulamov, S. O. Edgorov, M. Yu. Kratenko, S. L. Lutpulleev, K. T. Turdeliev, A. A. Yuldashev, and B. S. Yuldashev, 60-88 HEP (Tashkent preprint).

[43] V. V. Glagolev *et al.*, Sov. Jour. Nucl. Phys. **51**, 736(1990), in Russian.

[44] Yu. A. Troyan and V. N. Pechenov, Jour. of Nucl. Phys. **56**, 191 (1993), in Russian.

[45] V. V. Avdeichikov *et al.*, Jour. Nucl. Phys. **54**, 111 (1991), in Russian; Yu. A. Troyan *et al.*, Jour. Nucl. Phys. **54**, 1301 (1991), in Russian.

[46] V. B. Ganenko, V. A. Gushchin, Yu. V. Zhebrovskii, Yu. A. Kasatkin, L. Ya. Kolesnikov, S. I. Nagornyi, V. D. Ovchinnik, A. L. Rubashkin, P. V. Sorokin, and A. A. Zayats, JETP Letters **50**, 220 (1989), in Russian.

[47] B. Bock *et al.*, Nucl. Phys. **A459**, 573 (1986).

[48] L. A. Didenko *et al.*, JINR preprint E1-91-329; *ibid* E1-91-323.

[49] O. B. Abdinov, A. A. Baireamov, Yu. A. Boudagov, A. M. Dvornik, Yu. Ph. Lomakin, A. A. Mailov, V. B. Fliagin, and Yu. N. Khargeev, JINR Rapid Communications **15**, 34 (1986).

[50] C. Besliu, L. Popa, and V. Popa, J. Phys. **G18**, 807 (1992).

[51] C. Besliu *et al.*, JINR preprint, D1-85-433, in Russian.

[52] S. O. Edogorov *et al.*, FTI preprint 141-91, FVE Tashkent.

[53] H. Garcilazo, Phys. ReV. **C 52**, 1126 (1995).

[54] A. Faessler, A. J. Buchmann, M. I. Krivoruchenko, and B. V. Martemyanov, Phys. Lett. **B391**, 255 (1997); A. Faessler, A. J. Buchmann, M. I. Krivoruchenko and B. V. Martemyanov, J. Phys. G : Nucl. Part. Phys **24**, 791 (1998).

[55] V. B. Kopeliovich, Phys. of Atom. Nuclei **58**, 1327 (1995).

[56] A. Faessler, A. J. Buchmann, and H. I. Krivoruchenko Phys. ReV. **C 56**, 1576 (1997).

[57] N. K. Glendenning and J. Schaffner-Bielich, Phys. ReV. **C 58**, 1298 (1998).

[58] Chun Wa Wong, Phys. ReV. **C 57**, 1962 (1998).

[59] M. P. Combes *et al.*, Nucl. Phys. **A431**, 703 (1984).

[60] P. J. Mulders, A. T. Aerts, and J. J. de Swart Phys. Rev. **D 21**, 2653 (1980); Phys. Rev. **D 19**, 2635 (1979); Phys. Rev. Lett. **40**, 1543 (1978).

[61] The justification to include the deuteron in that quark clusters systematics, is that its short range part wave function can be considered as six-quark cluster.

[62] N. Konno, H. Nakamura, and H. Noya, Phys. ReV. **D 35**, 239 (1987); Phys. ReV. **D 37**, 154 (1988); Y. Uehara, N. Konno, H. Nakamura, and H. Noya, Nucl. Phys. **A606**, 357 (1996).

[63] A. Yokosawa, in *Proceedings of Sixth International Symposium on Polarization Phenomena in Nuclear Physics, Osaka, 1985*, edited by M.Kondo *et al.* J. Phys. Soc. Jpn. Suppl. **55**, 251 (1986).

[64] D. B. Lichtenberg, R. Roncaglia, and E. Predazzi, J. Phys. G : Nucl. Part. Phys. **23**, 865 (1997).

FIG. 1. Scatter plot of missing mass versus dibaryonic invariant mass events at T_p=1805 MeV, $\theta = 0.75^0$ lab.

FIG. 2. Number of events for dibaryonic M_{pX} invariant mass for two different cuts on the missing mass at T_p=1805 MeV, $\theta = 0.75^0$ lab.

FIG. 3. Cross sections for 1520 MeV incident protons versus the M_{pn} dibaryonic mass showing a small and narrow structure around 2050 MeV.

FIG. 4. Angular distribution of the dibaryonic structure observed at M_{pn}=2050 MeV for 1520 MeV incident protons and neutron missing mass.

FIG. 5. Part (a) shows the scatter plot of the raw data, and two circle arcs used to define a surface where only smooth corrections were applied. Part (b) shows the resulting M_{pX} distribution (see text). Part (c) shows the M_{pX} distribution when all data ($M_X \geq$960 MeV) was considered.

FIG. 6. Cross sections for 1520 MeV incident protons versus M_{pX} dibaryonic mass for missing masses $M_X \geq 960$ MeV. Straight lines are drawn at 2122 MeV.

FIG. 7. Analyzing power versus M_{pX} dibaryonic masses for data at 5^0 and 9^0 and 1520 MeV incident protons.

FIG. 8. Cross sections for 1805 MeV incident protons versus M_{pX} dibaryonic mass at 3.7^0. Cuts were introduced in order to remove the main part of the Δ n peak. However a tail remained which gave a peak around M_{pX}=2160 MeV. A large Δ Δ peak is observed around 2280 MeV.

FIG. 9. Cross sections for 2100 MeV incident protons against M_{pX} dibaryonic mass showing a dibaryonic structure at 2150 MeV.

FIG. 10. Cross sections for 2100 MeV incident protons versus M_{pX} dibaryonic mass showing a dibaryonic structure around 2230 MeV (vertical straight lines).

FIG. 11. Missing mass spectra for ^{3} He (p,d) X reaction showing the presence of a narrow dibaryon at M_X = 2122 MeV [11],[12].

FIG. 12. Masses of experimental narrow structures observed in previous experiments displayed versus the corresponding reference. The last column ($\star$) corresponds to the masses observed in this work.

FIG. 13. Experimental masses of narrow dibaryons (left) and masses calculated using the mass formula of equation 1. The numbers in brackets (right) indicate the two spin and isospin possible values for the two quark clusters.

FIG. 14. Masses of narrow dibaryons. From left to right : experimental results, calculated results using the $q^2 - q^4$ clusters mass formula (1) and values found using the narrow baryonic masses.

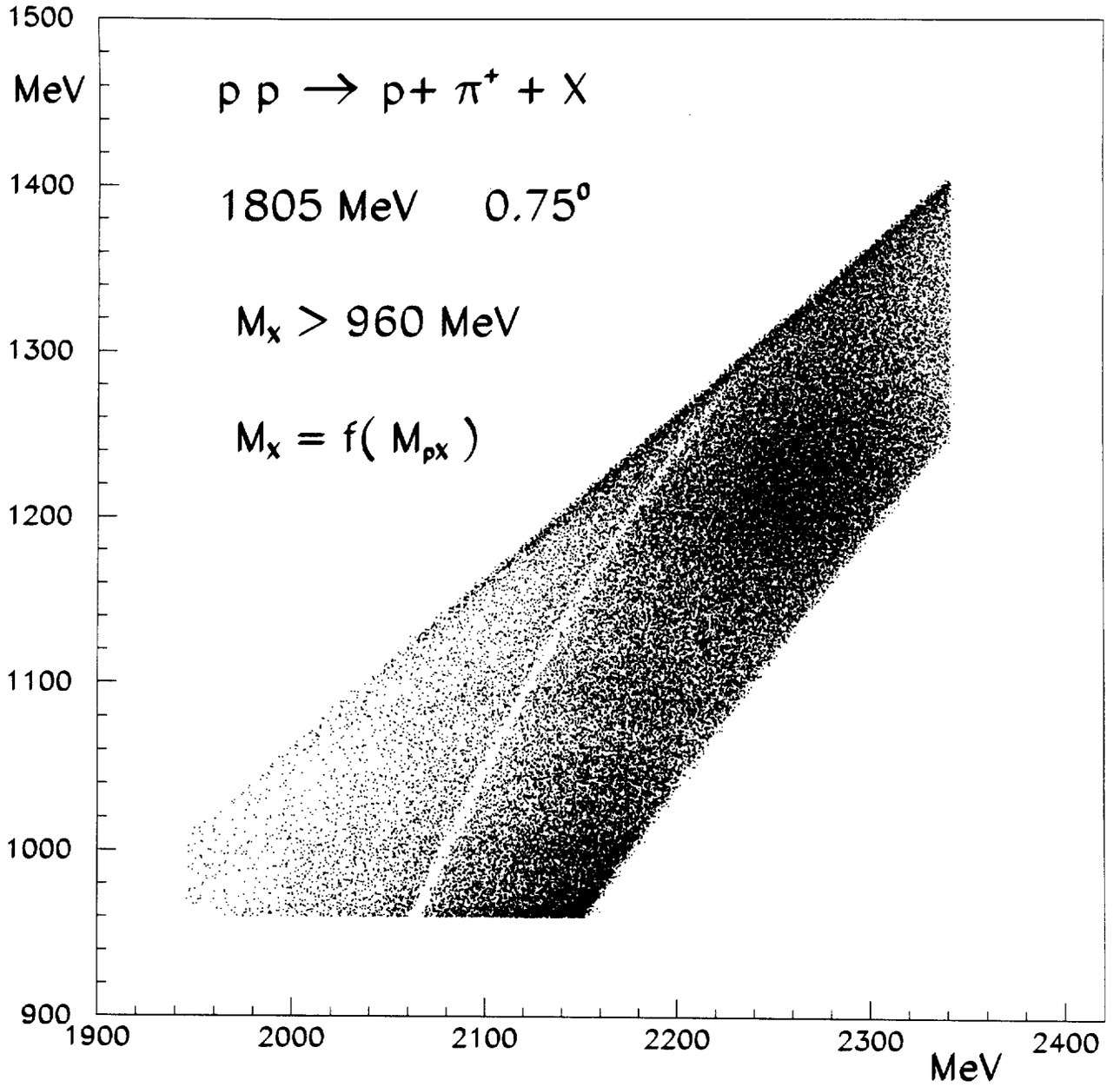
1500
MeV
1400
1300
1200
1100
1000
900
p p → p+ π+ + X
1805 MeV 0.75°
Mx > 960 MeV
Mx = f(Mpx)
1900
2000
2100
2200
2300
2400
MeV

Figure 1

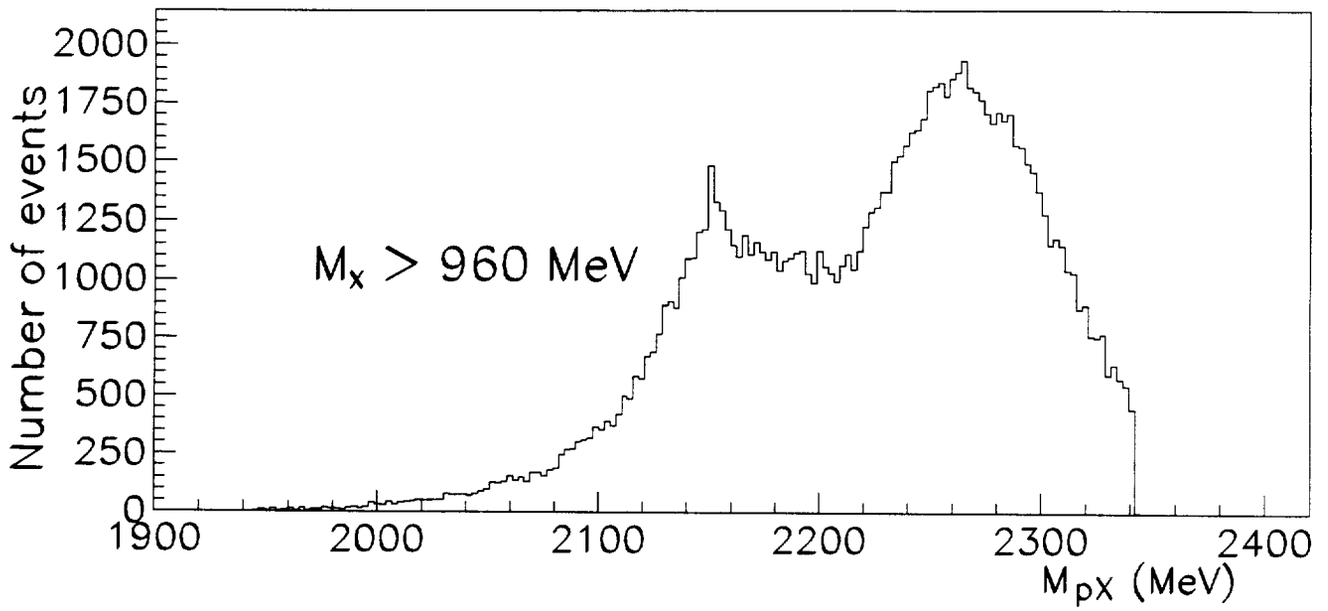
Number of events
2000
1750
1500
1250
1000
750
500
250
0
$M_x > 960$ MeV
1900
2000
2100
2200
2300
2400
M_{pX} (MeV)

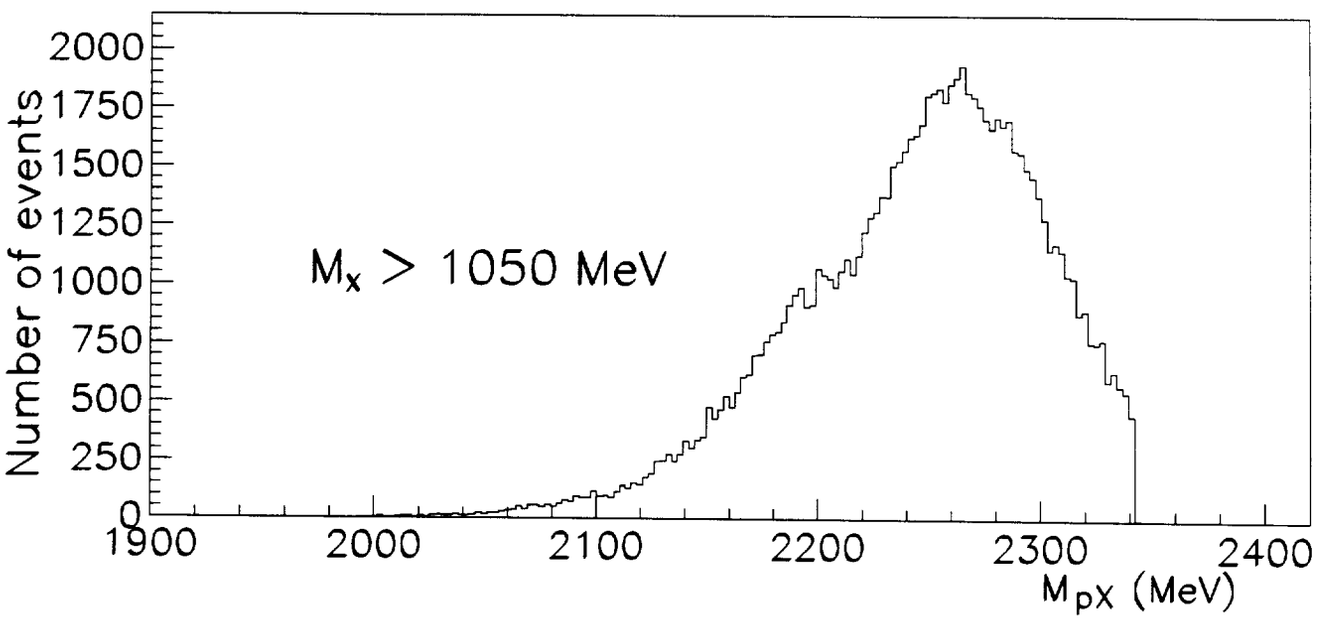
Number of events
2000
1750
1500
1250
1000
750
500
250
0
$M_x > 1050$ MeV
1900
2000
2100
2200
2300
2400
M_{pX} (MeV)

Figure 2

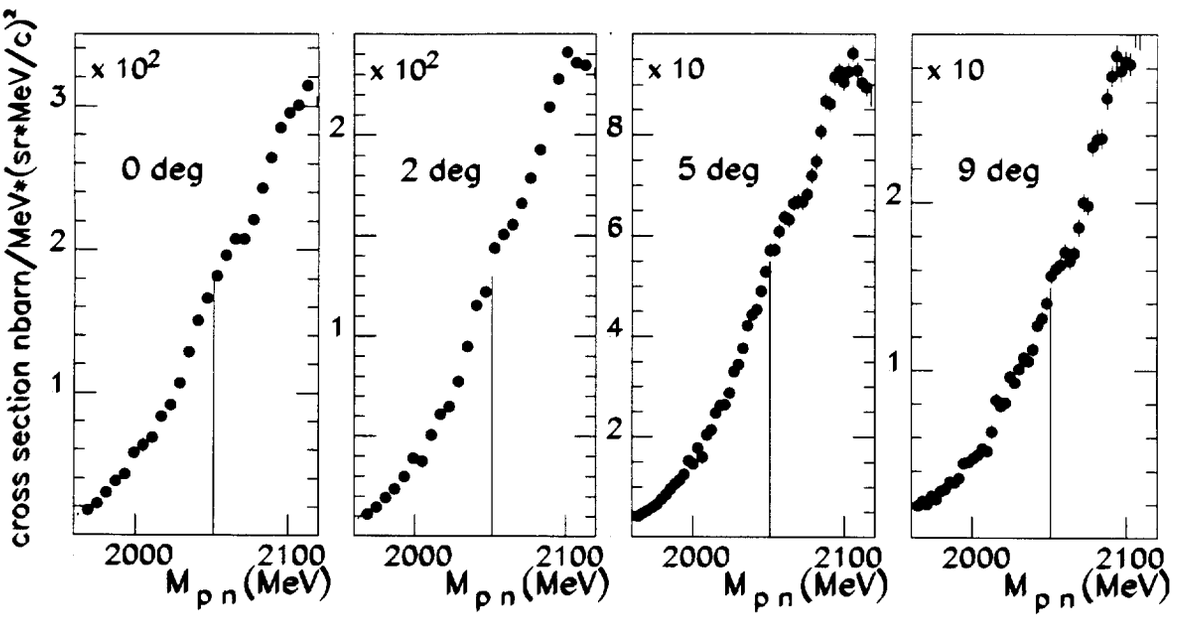
cross section nbarn/MeV*(sr*MeV/c)²
x 10²
0 deg
x 10²
2 deg
x 10
5 deg
x 10
9 deg
2000
2100
M p n (MeV)

Figure 3

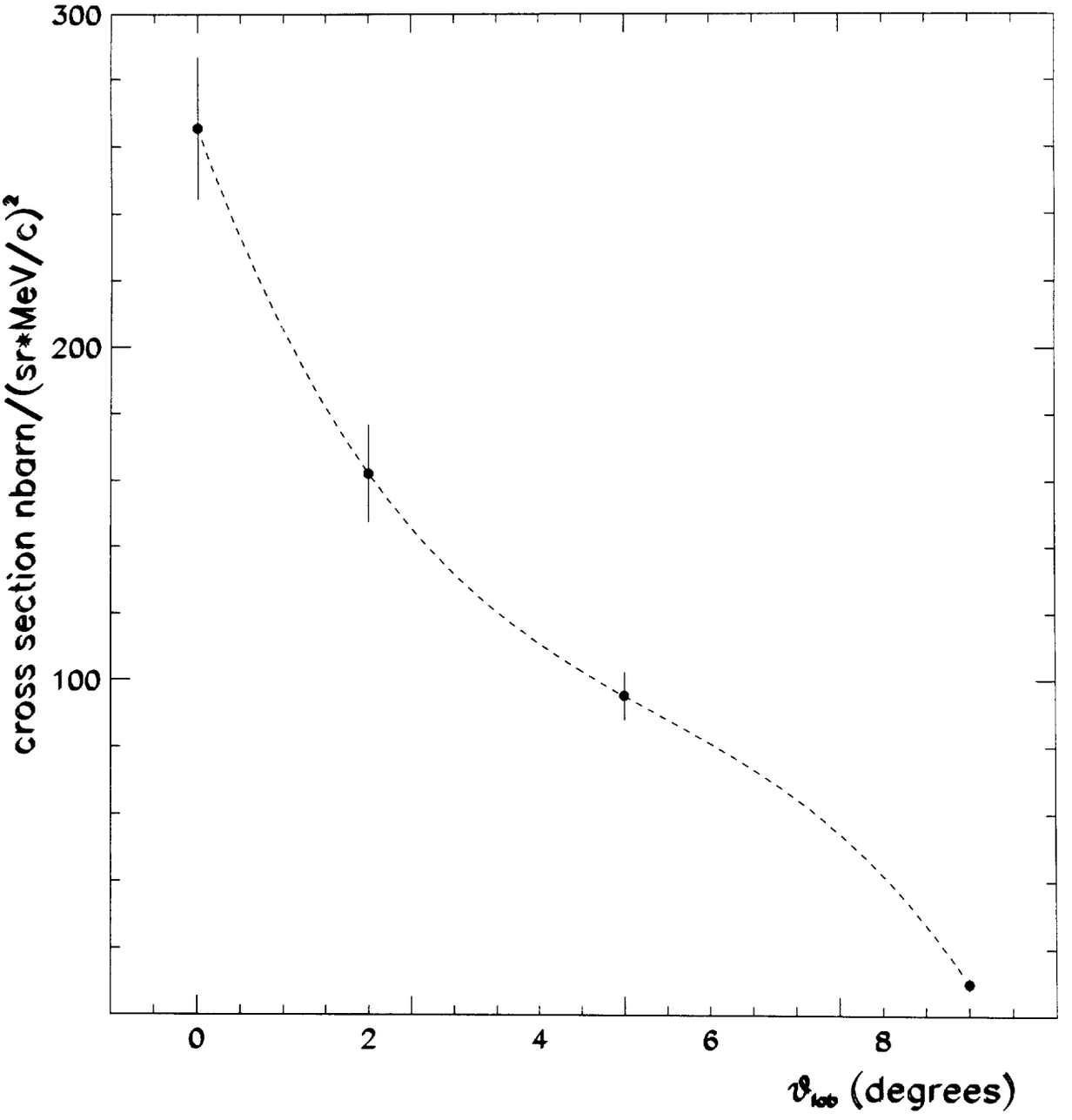

Figure 4

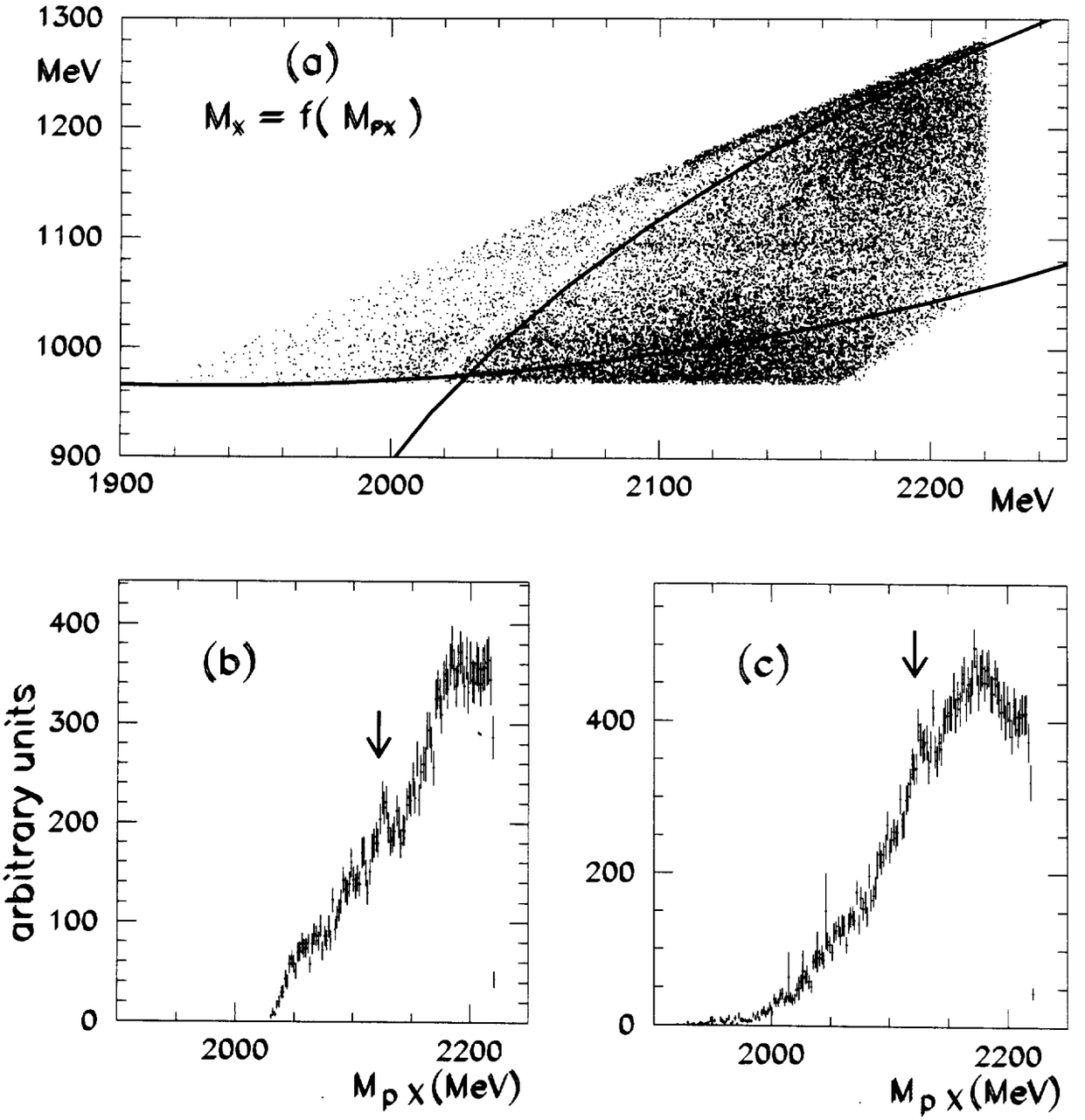
(a)
$M_X = f(M_{PX})$
1300
MeV
1200
1100
1000
900
1900
2000
2100
2200
MeV
(b)
(c)
arbitrary units
400
300
200
100
0
2000
2200
$M_{p\,X}$ (MeV)

Figure 5

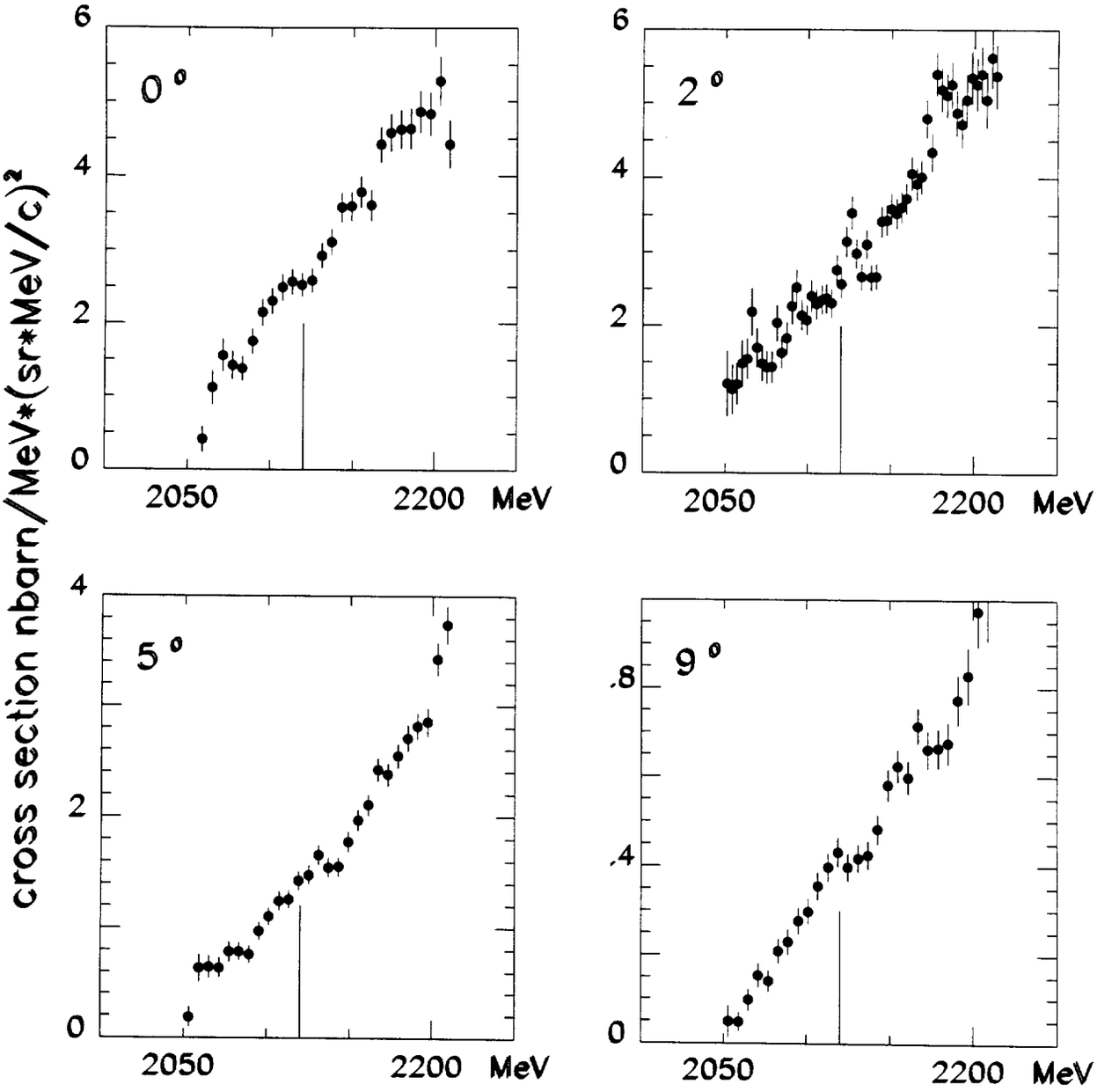

Figure 6

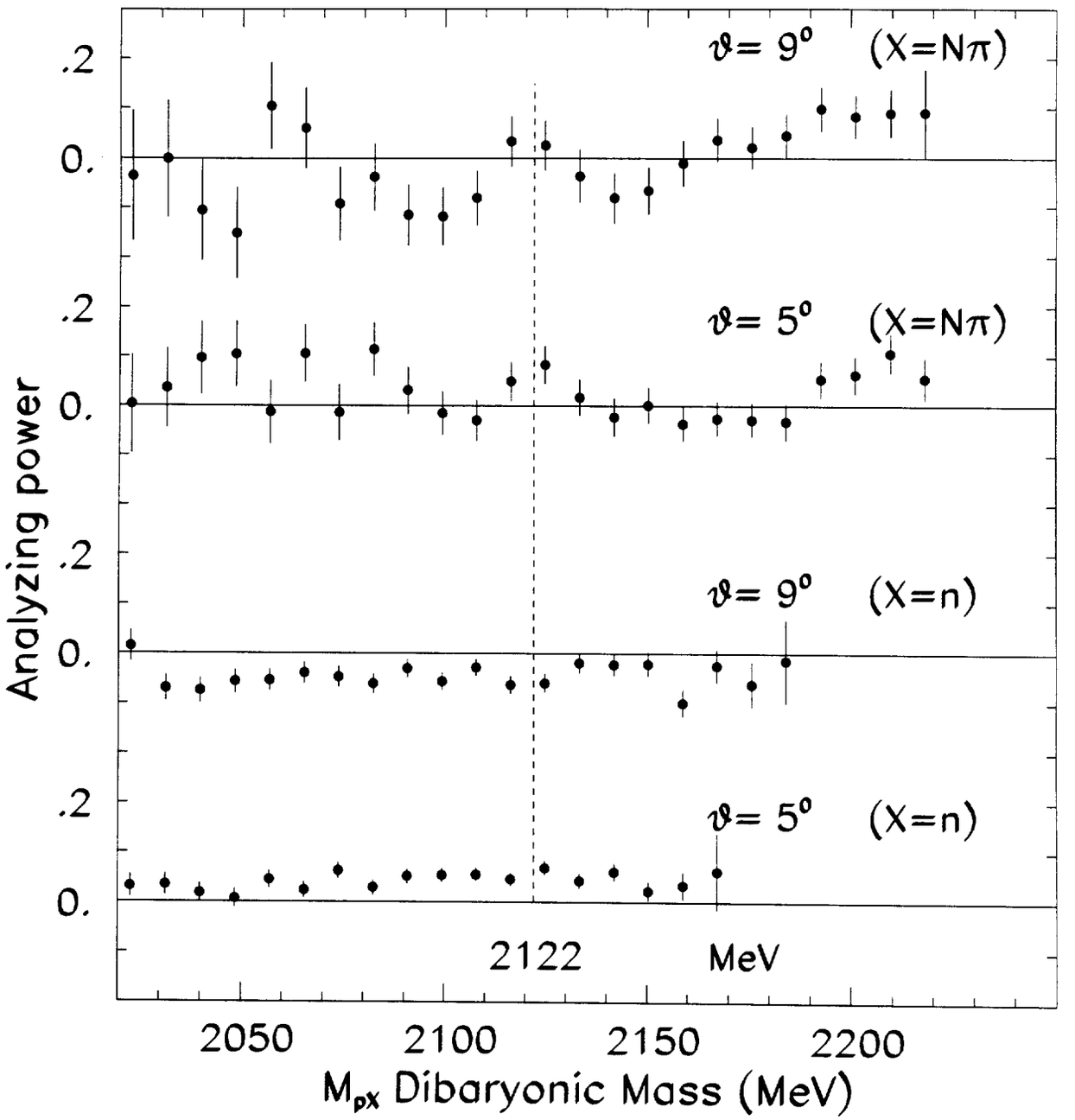
.2
0.
.2
0.
.2
0.
.2
0.
Analyzing power
ϑ= 9° (X=Nπ)
ϑ= 5° (X=Nπ)
ϑ= 9° (X=n)
ϑ= 5° (X=n)
2122 MeV
2050
2100
2150
2200
M_pX Dibaryonic Mass (MeV)

Figure 7

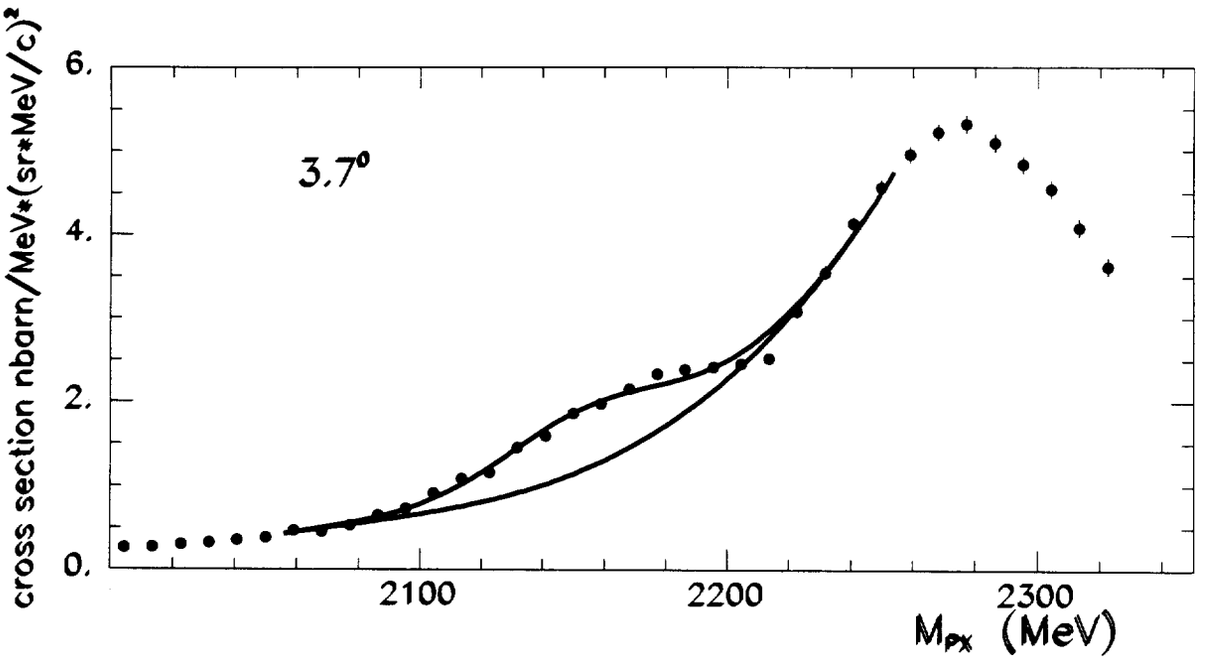
cross section nbarn/MeV*(sr*MeV/c)²
6.
4.
2.
0.
3.7°
2100
2200
2300
M_PX (MeV)

Figure 8

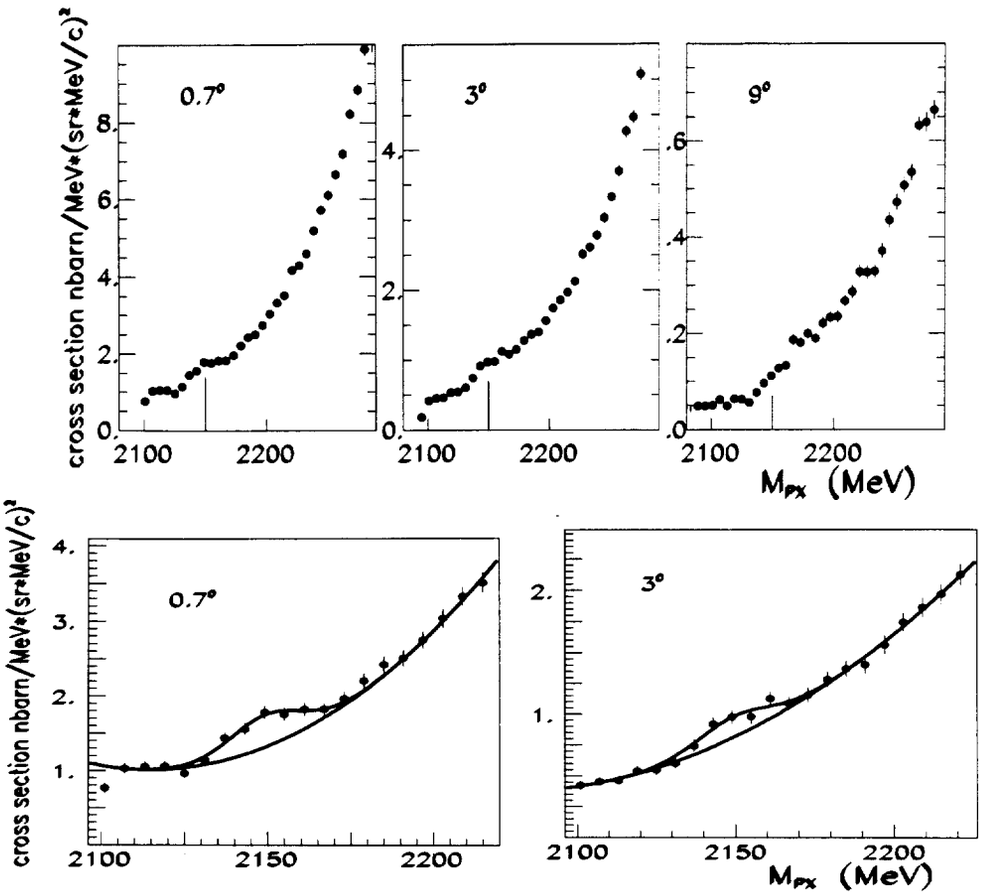
cross section nbarn/MeV*(sr*MeV/c)²
0.7°
3°
9°
2100
2200
M_PX (MeV)

cross section nbarn/MeV*(sr*MeV/c)²
0.7°
3°
2100
2150
2200
M_PX (MeV)

Figure 9

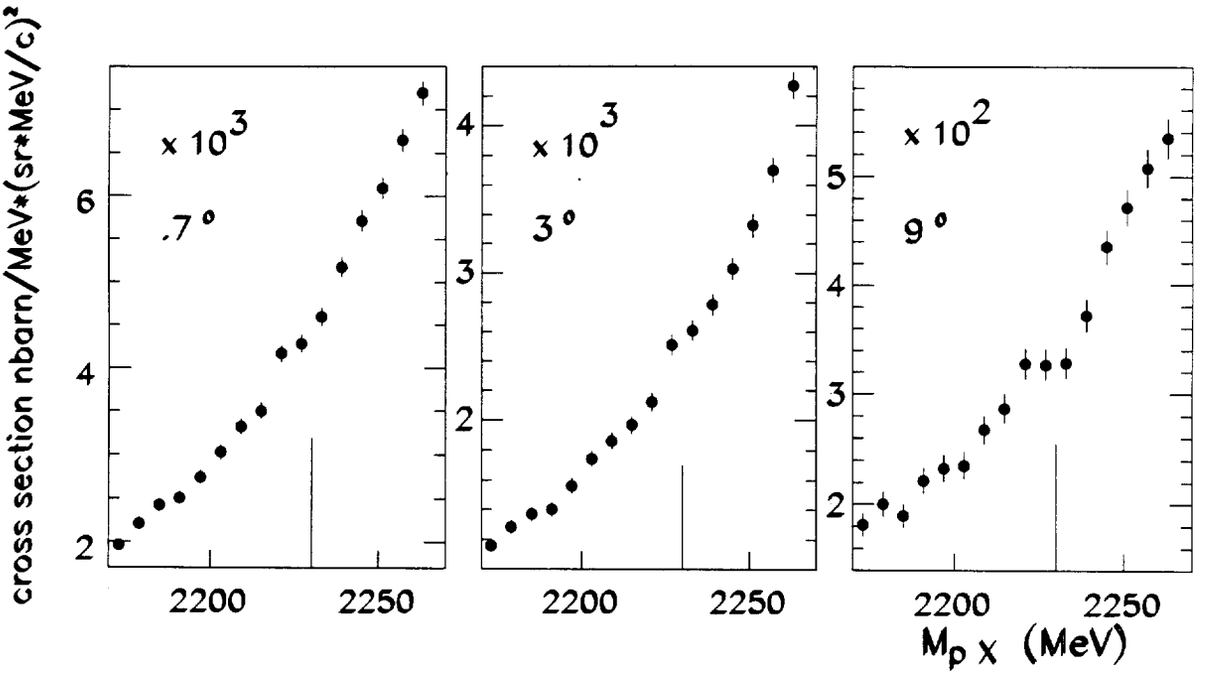
cross section nbarn/MeV*(sr*MeV/c)²
x 10³
7°
x 10³
3°
x 10²
9°
2200
2250
2200
2250
2200
2250
M_p X (MeV)

Figure 10

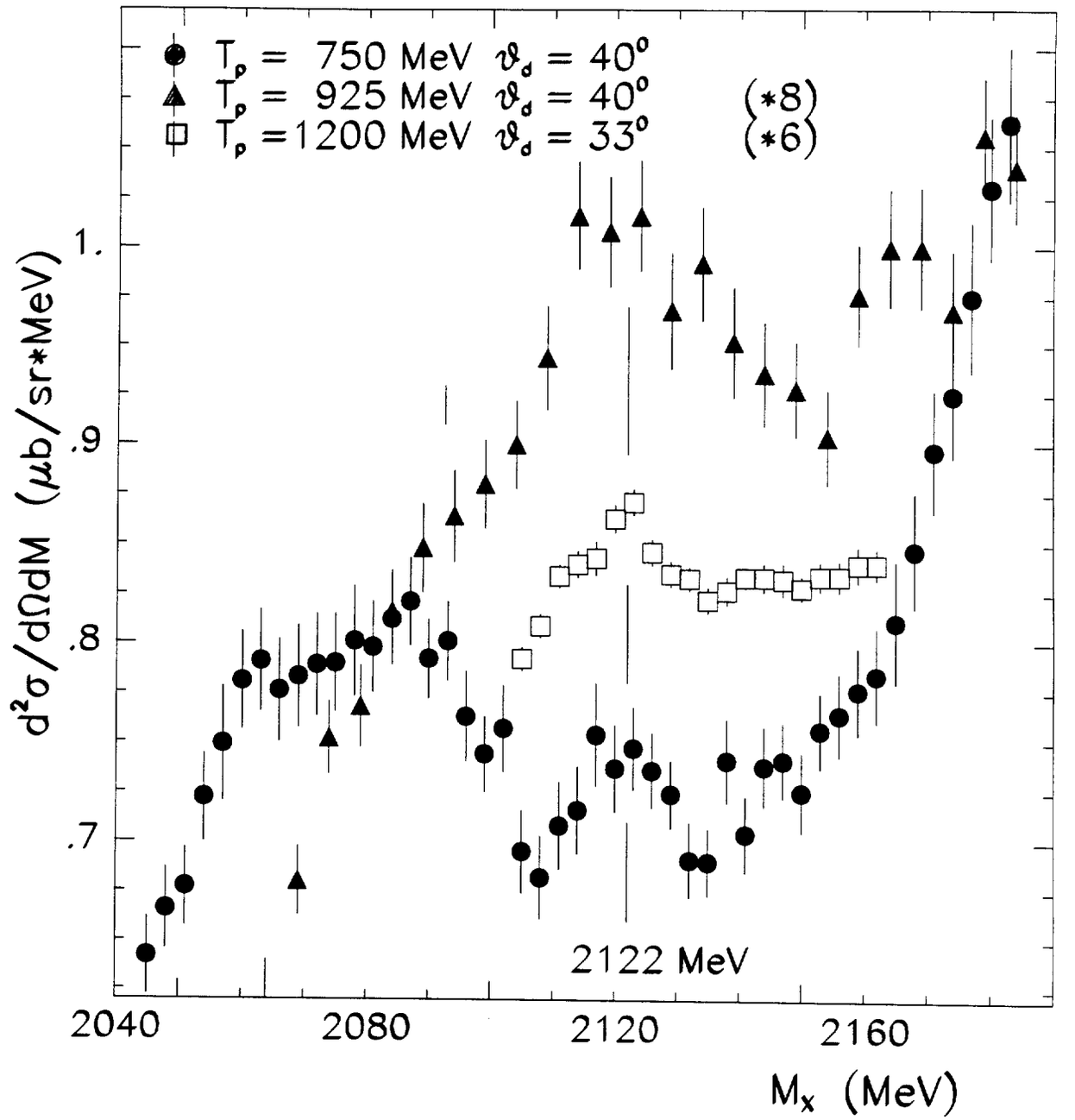
T_p = 750 MeV ϑ_d = 40°
T_p = 925 MeV ϑ_d = 40°
T_p =1200 MeV ϑ_d = 33°
(*8)
(*6)
$d^2\sigma/d\Omega dM$ (μb/sr*MeV)
1.
.9
.8
.7
2122 MeV
2040
2080
2120
2160
M_x (MeV)

Figure 11

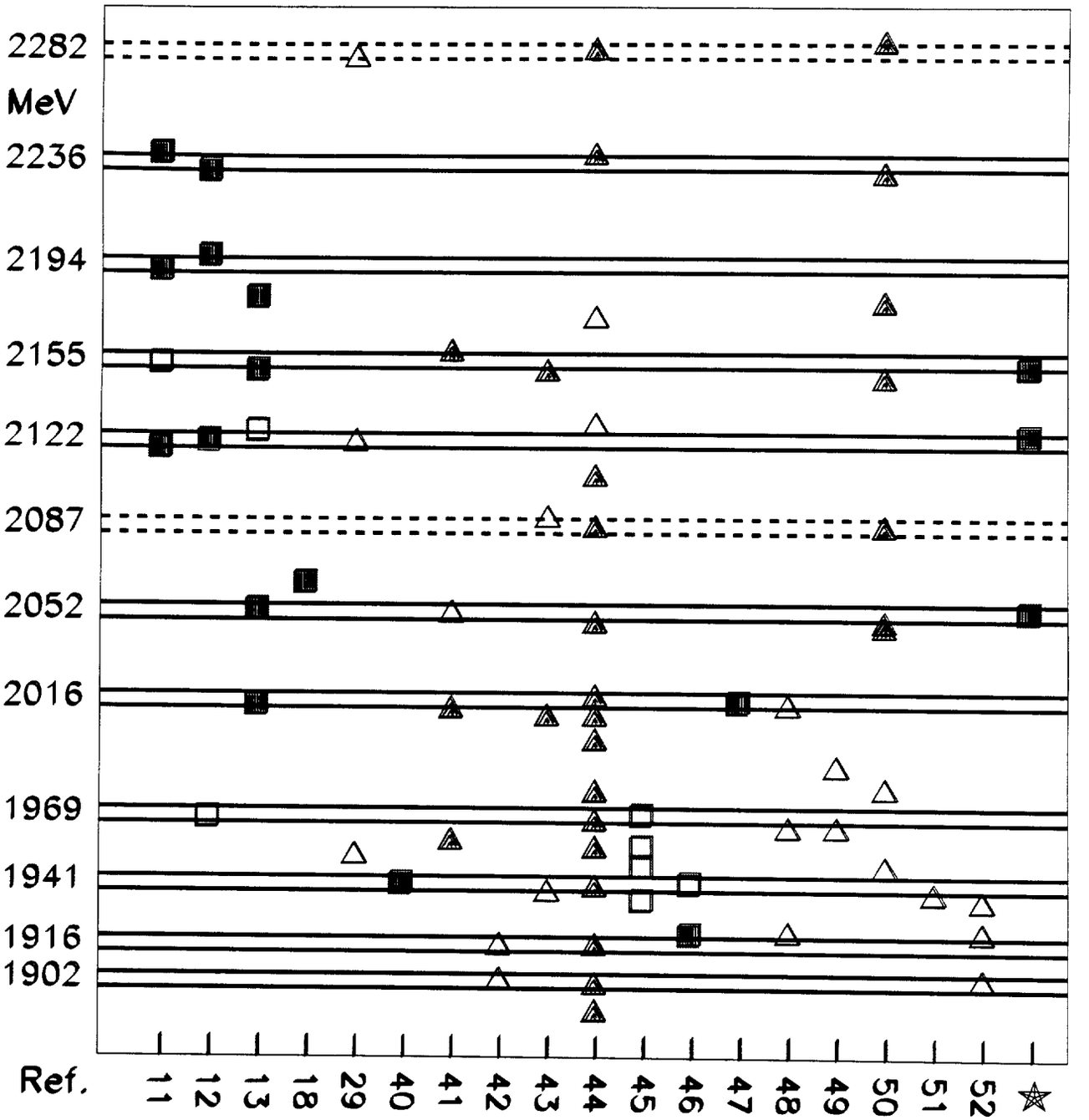
2282
MeV
2236
2194
2155
2122
2087
2052
2016
1969
1941
1916
1902
Ref.
11
12
13
18
29
40
41
42
43
44
45
46
47
48
49
50
51
52

Figure 12

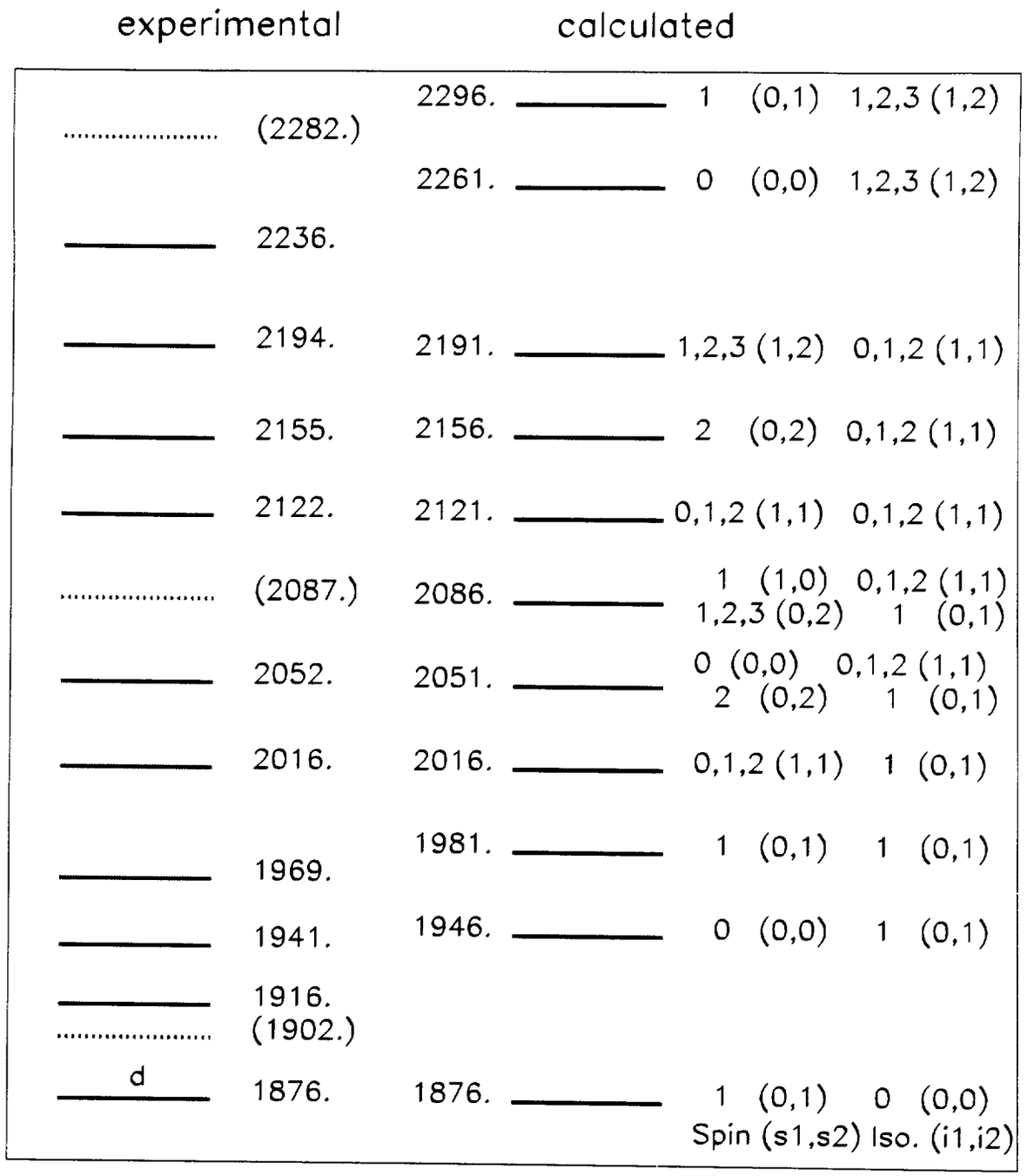
experimental
calculated
(2282.)
2296.
1 (0,1) 1,2,3 (1,2)
2261.
0 (0,0) 1,2,3 (1,2)
2236.
2194.
2191.
1,2,3 (1,2) 0,1,2 (1,1)
2155.
2156.
2 (0,2) 0,1,2 (1,1)
2122.
2121.
0,1,2 (1,1) 0,1,2 (1,1)
(2087.)
2086.
1 (1,0) 0,1,2 (1,1)
1,2,3 (0,2) 1 (0,1)
2052.
2051.
0 (0,0) 0,1,2 (1,1)
2 (0,2) 1 (0,1)
2016.
2016.
0,1,2 (1,1) 1 (0,1)
1981.
1 (0,1) 1 (0,1)
1969.
1941.
1946.
0 (0,0) 1 (0,1)
1916.
(1902.)
d
1876.
1876.
1 (0,1) 0 (0,0)
Spin (s1,s2) Iso. (i1,i2)

Figure 13

ISOVECTOR DIBARYONIC MASSES (MEV)

Experimental	calculation using q2–q4 clusters	calculation using narrow baryons
2194	2191	2188
2155	2156	
		2138
2122	2121	
		2098
(2087)	2086	2088
2052	2051	2048
		2032
2016	2016	
		2008
	1981	1982
1969		
1941	1946	1942
1916		
(1902)		
d 1876	1876	1876

Figure 14